# Life on the Move: Modeling the Effects of Climate-Driven Range Shifts with Integrodifference Equations

**Ying Zhou and Mark Kot**

**Abstract** Climate change is causing many species to shift their ranges. We analyze an integrodifference equation that combines growth, dispersal, and a shifting habitat in order to assess the impact of climate change on persistence. We apply this model to butterflies and show that over-dispersal and under-dispersal can both lead to extinction. We focus on the critical range-shift speed (for extinction), survey numerical methods for determining this speed, and introduce new analytic approximations for the critical shift speed. Finally, we apply our numerical methods and analytic approximations to a variety of redistribution kernels and show that critical-speed curves shed light on the complicated effects of dispersal on persistence in a changing climatic environment.

## 1 Introduction

The geographic ranges of wildlife species are constantly responding to changes in climate. Paleoecological studies have documented extensive species range changes during the glacial and interglacial alternations in the Quaternary Period [12, 32]. More recently (1956–2005), the Earth has been warming up at the rate of 0.13 °C/decade [34]. Species were expected to shift their ranges during this period, and this has now been documented [13, 29, 39, 49, 70, 71].

One major difference between the current warming event and earlier climatic changes in the Quaternary is that modern anthropogenic activities have created obstacles that make it difficult for the Earth's biota to survive climate change. Species need to shift their ranges to avoid excessive habitat loss during climate change, but, unlike organisms hundreds of thousands of years ago, species now face

Y. Zhou (✉) · M. Kot
Department of Applied Mathematics, University of Washington, Box 352420, Seattle, WA, USA
e-mail: yzhou@amath.washington.edu; mark_kot@comcast.net

M.A. Lewis et al. (eds.), *Dispersal, Individual Movement and Spatial Ecology*, Lecture Notes in Mathematics 2071, DOI 10.1007/978-3-642-35497-7_9,

severe habitat fragmentation that makes shifting their ranges difficult [30, 64, 78]. Invasive exotics introduced by anthropogenic activities further stress indigenous species, since a changing climate creates new opportunities for invasive species to compete with native species. In general, ecologists must now assess the spatial effects of multiple factors in planning conservation strategies. They must, in particular, determine how multiple factors affect species ranges.

Many quantitative tools help us estimate future range shifts. For example, correlation models such as climate envelope models have been used to predict ranges for various climate change scenarios [4, 25, 36]. These models typically correlate species ranges with climatic variables using statistical tools, and then estimate potential ranges by combining correlational information with projections of future climate. These models cannot, however, easily integrate population dynamics, such as growth, dispersal, and interspecific interactions.

Other mathematical models have been used to bridge this gap. Travis [87] and Best et al. [7] used stochastic, spatially explicit, patch occupancy models to study the effects of range-shift speed on persistence. Potapov and Lewis [72] and Berestycki et al. [5], in turn, used deterministic reaction–diffusion models to study this topic. Reaction–diffusion equations are particularly suitable for organisms with continuous and simultaneous growth and dispersal.

For many organisms, growth and dispersal are discrete episodes in the life cycle. Consider, for example, Edith's checkerspot butterfly (*Euphydryas editha*). In the San Francisco Bay area of California, eggs of this species hatch in April and the larvae feed and develop for 10–14 days. The larvae then enter diapause [27]. Post-diapause larvae feed and grow from December to February. They then pupate and emerge as adults [27]. The adults of *E. editha*, which live some 10 days, emerge, fly, mate, search for oviposition sites, and complete their life cycle in March and April [61]. For this univoltine species, adults are the primary dispersers; their dispersal occurs during a very narrow window of time.

The mortality rate of *E. editha*'s larvae depends on synchrony between their life cycle and that of their host plants: larvae must reach their fourth instar and enter diapause before their host plants senesce [67]. This synchrony is strongly affected by climatic variables such as temperature and precipitation [67]. As a result, the population dynamics of *E. editha* are sensitive to climate change. Parmesan [66] examined populations of *E. editha* throughout its range and found that populations along its southern range boundary suffered extinction rates four times higher than those along its northern range boundary. Population extinction rates at lower elevations, meanwhile, were nearly three times as high as those at higher elevations. These drastic differences in extinction rates clarify why the mean location of *E. editha* populations shifted northward and upward [67].

Many other examples of organisms with discrete growth and dispersal occur in the range-shift literature. For these species, population dynamics are more easily described using discrete-time models. We therefore attack the problem of climate-induced range shifts using integrodifference equations (IDEs). IDEs are discrete-time, continuous-space models that combine growth and dispersal [28,41,42,47,51,

54, 55, 62, 63, 88]. In this chapter, we will describe and analyze an IDE model that includes climate-driven spatial shifts.

In Sect. 2, we describe our basic model, apply it to butterflies, and show how over-dispersal and under-dispersal can both lead to extinction. In Sect. 3, we introduce the critical range-shift speed and reduce the problem of finding this speed to an eigenvalue problem. In Sect. 4, we survey numerical approaches for solving this problem. In Sects. 5 and 7, we use Legendre series and Taylor series to obtain analytic approximations of the critical shift speed. We apply our numerical and analytic approximations to a toy problem, in Sect. 6, and to more realistic kernels, in Sect. 8. Finally, we summarize and discuss our results in Sect. 9.

## 2 Is Further Better?

Several recent studies suggest that traits such as dispersal ability affect whether a species can successfully shift its range [11, 20, 65, 75, 77, 86]. For example, Pöyry et al. [73] related observed range shifts of butterflies in Finland to 11 butterfly life-history traits, such as mobility, habitat, and host-plant form. They found that habitat availability and dispersal capacity were the two traits most likely to determine whether a butterfly could keep up with climate change by shifting its range.

There is little argument that a sedentary species with little habitat has poor prospects in a world of climate change. But how about a vagile species whose habitat is shifting and fragmenting as we speak? What are its prospects? And, does higher dispersal ability always lead to greater success? We attempt to answer these questions by applying a recently developed IDE model [93] to butterflies.

Without loss of generality, let us assume that we have a univoltine butterfly that thrives on a suitable, spatially continuous patch of habitat in the Northern Hemisphere. Since ranges are expected to shift polewards, we will assume that this patch is a strip or zone bounded by lines of latitude. For mathematical simplicity, we reduce this strip to the one-dimensional interval $[-L/2, L/2]$. The length of this interval, $L$, in kilometers, represents the patch size. We assume that climate change shifts the two zonal boundaries northwards, at the speed of $c$ km/year. Thus, $t$ years after the initial time point, the suitable patch is located at $[-L/2 + ct, L/2 + ct]$.

Because the butterfly is univoltine and has well-defined life stages, we can keep track of the population dynamics by censusing the population once a year. If we label the density of freshly oviposited eggs in year $t$ at location $x$ as $n_t(x)$, then the density of eggs in the next year can be written as

$$n_{t+1}(x) = \int_{-\frac{L}{2}+ct}^{\frac{L}{2}+ct} k(x, y)\, f\,[n_t(y)]\, dy. \tag{1}$$

The formulation of (1) can be understood by going through the butterfly's life cycle. Most of the life cycle, from egg hatching to pupal eclosion, is a

relatively sedentary stage. The function $f$ describes growth during this stage. It maps the density of eggs (on plants) to a new density of eggs (in emerging adults). To construct the growth function $f$ we might, for example, consider density dependence, larval mortality, clutch size, etc. In this paper, we will use the Beverton–Holt [8] recruitment curve,

$$f(n_t) = \frac{R_0 n_t}{1 + [(R_0 - 1)/K]\, n_t}, \tag{2}$$

as our growth function. Here, $R_0 = f'(0)$ is the net reproductive rate and $K$ is the carrying capacity.

The adult butterflies are the dispersal stage. Eggs produced at $y$ are carried to location $x$ with some probability. For a fixed source of eggs $y$, we think of the redistribution kernel, $k(x, y)$, as a probability density function for the destination $x$ of propagules. The kernel may depend on only the difference between $x$ and $y$. In this case, we have a difference kernel, $k(x, y) = k(x - y)$, and we may think of $k(x - y)$ as the probability density function for the displacement (rather than the destination). Kernels can be estimated from mark-release-recapture studies.

Unfortunately, ecologists often lack detailed dispersal data for butterflies. As a result, comparative studies of butterflies often assume mobilities based on expert opinion [17, 40, 73, 84]. Recently, however, Stevens et al. [84] performed a meta-analysis of butterfly studies and summarized dispersal data. They showed that distributions of dispersal distances could be fit with negative exponential curves. These curves engender a 2D probability density function for the deposition of propagules [15, 16]. By taking the marginal distribution of this 2D kernel [51], we obtained [94] the 1D redistribution kernel

$$k(x - y) = \frac{\alpha}{\pi} K_0 (\alpha |x - y|), \tag{3}$$

for butterflies, where $K_0(x)$ is the modified Bessel function of the second kind of order zero. The parameter $\alpha$, the reciprocal of the mean dispersal distance, ranges from $0.76\,\mathrm{km}^{-1}$ for vagile species to $24.25\,\mathrm{km}^{-1}$ for sedentary species [84].

In model (1), eggs hatch and grow and adults emerge if they are in the climate-shifted patch for year $t$. Adults then oviposit their eggs both inside and outside the patch. Equation (1) tallies the movement of propagules from sources $y$ within the patch to obtain the density of eggs, $n_{t+1}(x)$, at the start of the next generation.

To explore the effects of dispersal on survival, we numerically iterated equation (1) with growth function (2) and redistribution kernel (3). We set the net reproductive rate, the patch size, and the shift speed to the values $R_0 = 1.9$, $L = 0.5\,\mathrm{km}$, and $c = 0.1\,\mathrm{km/year}$. We then chose three values of $\alpha$ from across the spectrum of observed values [84]. Figure 1a–c show the dynamics of the three populations. Populations die out for high ($\alpha = 12\,\mathrm{km}^{-1}$) and low ($\alpha = 2.5\,\mathrm{km}^{-1}$) values of $\alpha$. They survive for intermediate $\alpha$ ($\alpha = 6\,\mathrm{km}^{-1}$).

The causes of the extinctions for high and low $\alpha$ differed. The highly sedentary population ($\alpha = 12\,\mathrm{km}^{-1}$) in Fig. 1a was limited by its dispersal ability. It simply

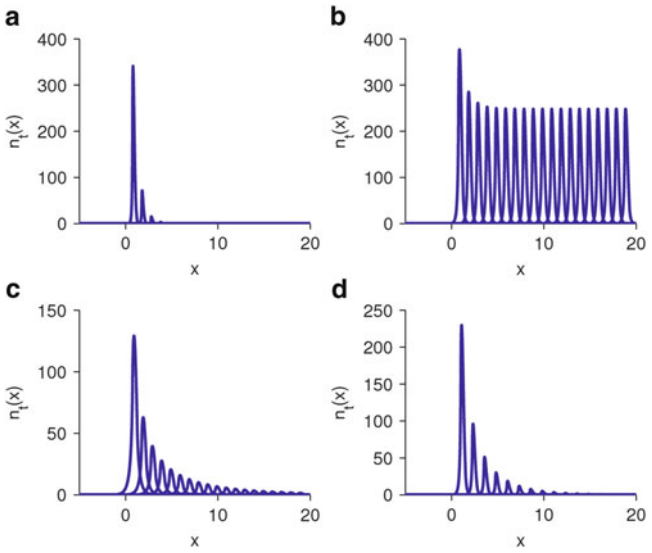


**Fig. 1** Simulations of IDE (1) with growth function (2) and kernel (3) show that a species' ability to survive climate change depends on both its dispersal ability and the speed of climate change. For shift speed $c = 0.1\,\text{km/year}$, (**a**) a sedentary population ($\alpha = 12\,\text{km}^{-1}$) cannot keep up with its shifting habitat and goes extinct; (**b**) an intermediate population ($\alpha = 6\,\text{km}^{-1}$) survives; (**c**) a vagile population ($\alpha = 2.5\,\text{km}^{-1}$) over-disperses and goes extinct. For $c = 0.125\,\text{km/year}$, (**d**) the intermediate population ($\alpha = 6\,\text{km}^{-1}$) also goes extinct. For all four subfigures, $L = 0.5\,\text{km}$, $R_0 = 1.9$, and $K = 1,000$. The initial distribution was $n_0(x) = K\exp(-x^2/2)$. The distribution is displayed every ten generations and was computed using an FFT-assisted implementation of the extended trapezoidal rule with $2^{16}$ nodes

could not keep up with its shifting habitat. In contrast, the vagile population ($\alpha = 2.5\,\text{km}^{-1}$) in Fig. 1c over-dispersed and was patch-size (or growth-rate) limited [see also 93, Fig. 5]. Thus, climate change and habitat fragmentation can both be important. Conservation efforts need to integrate both factors.

## 3 The Critical Range-Shift Speed

Instead of comparing species traits, let us now take a different perspective and look at the severity of climate change. Even if the population in Fig. 1b is doing fine, will it still prosper if the shift speed $c$ is increased? No! Figure 1d demonstrates that our population collapses if we raise the shift speed to $c = 0.125\,\text{km/year}$.

The shift speed $c$ clearly has an important effect on the viability of our population. Numerical simulations suggest that for each growth rate, patch size, and redistribution kernel, there may be a critical shift speed $c^*$ beyond which the population goes extinct. We will now employ some simple mathematical analyses to determine this critical shift speed.

Consider (1) with a difference kernel,

$$n_{t+1}(x) = \int_{-\frac{L}{2}+ct}^{\frac{L}{2}+ct} k(x-y)\, f\,[n_t(y)]\, dy. \tag{4}$$

For convenience, we will now assume, throughout the remainder of this paper, that our growth curve is nonnegative, monotonically increasing, and that it satisfies

$$f(n) \leq f'(0)n, \tag{5}$$

for $n \geq 0$. In particular, we explicitly exclude Allee effects [1]. These conditions are certainly satisfied by Beverton–Holt curve (2) for $R_0 > 1$.

Since the patch moves with constant speed $c$, we will look for steady states in the moving frame of the patch. This means we will look for moving pulses of the form

$$n_t(x) = n^*(x - ct). \tag{6}$$

Using this ansatz,

$$n_{t+1}(x) = n^*(x - ct - c). \tag{7}$$

Substituting (6) and (7) into (4), we find that the moving pulse satisfies

$$n^*(x - ct - c) = \int_{-\frac{L}{2}+ct}^{\frac{L}{2}+ct} k(x-y)\, f[n^*(y - ct)]\, dy. \tag{8}$$

Rewriting (8) in terms of the shifted spatial variables $\bar{x} = x - ct$ and $\bar{y} = y - ct$, we obtain

$$n^*(\bar{x} - c) = \int_{-\frac{L}{2}}^{\frac{L}{2}} k(\bar{x} - \bar{y})\, f\left[n^*(\bar{y})\right]\, d\bar{y}. \tag{9}$$

Shifting $\bar{x}$ by $c$, we find that moving pulse $n^*(\bar{x})$ is a solution of the equation

$$n^*(\bar{x}) = \int_{-\frac{L}{2}}^{\frac{L}{2}} k(\bar{x} + c - \bar{y})\, f\left[n^*(\bar{y})\right]\, d\bar{y}. \tag{10}$$

For this derivation to work, our kernel must be a difference kernel.

It is hard, in general, to find closed-form solutions $n^*(\bar{x})$ of (10). We can, however, identify special solutions in special cases. If the growth curve $f$ has the trivial solution as a fixed-point, then

$$n^*(\bar{x}) \equiv 0 \tag{11}$$

is a solution of (10).

For the simple growth functions that we are using, we expect persistence to be equivalent to instability of solution (11) (no bistability). To study the stability of a moving pulse, we add a small, localized perturbation $\xi_t(x)$ to the pulse,

$$n_t(x) = n^*(\bar{x}) + \xi_t(x). \tag{12}$$

We then substitute $n_t(x)$ into integrodifference equation (4), linearize about $n^*(\bar{x})$,

$$\xi_{t+1}(x) = \int_{-\frac{L}{2}+ct}^{\frac{L}{2}+ct} k(x-y)\, f'\left[n^*(\bar{y})\right] \xi_t(y)\, dy, \tag{13}$$

and study the growth of the perturbation. Equation (13) is difficult to analyze in general, but luckily, for the trivial solution, $f'[n^*(\bar{y})] = f'(0)$ is a constant. As a result, (13) now reduces to

$$\xi_{t+1}(x) = R_0 \int_{-\frac{L}{2}+ct}^{\frac{L}{2}+ct} k(x-y)\, \xi_t(y)\, dy, \tag{14}$$

where $R_0 = f'(0)$ is the net reproductive rate.

Since we are interested in perturbations that persist in the moving frame, we now focus on perturbations that can be written as a product of a growth term $\lambda^t$ and a traveling term $u(x-ct)$,

$$\xi_t(x) = \lambda^t\, u(\bar{x}) \equiv \lambda^t\, u(x-ct). \tag{15}$$

It now follows that

$$\lambda\, u(\bar{x}) = R_0 \int_{-\frac{L}{2}}^{\frac{L}{2}} k(\bar{x}+c-\bar{y})\, u(\bar{y})\, d\bar{y}. \tag{16}$$

Finally, for notational convenience, but at great risk of confusing the reader, we drop the bars on $\bar{x}$ and $\bar{y}$,

$$\lambda\, u(x) = R_0 \int_{-\frac{L}{2}}^{\frac{L}{2}} k(x+c-y)\, u(y)\, dy. \tag{17}$$

This is the key equation in this paper; we will use it to determine the critical speed $c^*$. It is a homogeneous Fredholm integral equation of the second kind. Please keep in mind, however, that the $x$ and $y$ in this equation are actually in the moving frame of the habitat. That is, they are really the barred variables.

Equation (17) can also be rewritten as the operator equation,

$$\lambda u(x) = K[u(x)], \tag{18}$$

where $K$ is the linear operator

$$K: \qquad u(x) \quad \rightarrow \quad R_0 \int_{-\frac{L}{2}}^{\frac{L}{2}} k(x+c-y)\, u(y)\, dy. \tag{19}$$

The parameter $\lambda$ is an eigenvalue of the operator, while $u(x) \neq 0$ is the corresponding eigenfunction. In general, this eigenvalue problem is nasty, but if the operator $K$ is compact (or completely continuous), the problem simplifies. The eigenvalues of a compact linear operator form a discrete set, the point spectrum $\Lambda = \{\lambda_0, \lambda_1, \lambda_2, \ldots\}$. This set may be finite, countably infinite, or empty [33, 38]. Each eigenvalue has finite multiplicity and eigenvalues can only accumulate at zero. Compact operators are, in many ways, similar to matrices.

What do we need for $K$ to be compact? It helps if the domain of our problem is closed and bounded. So, for mathematical convenience, let us now impose the restriction that $x \in [-L/2, L/2]$ and $y \in [-L/2, L/2]$ for finite $L$. In addition, it also helps if our kernel $k(x-y)$ is a continuous function [44] or, more generally, if $k(x-y)$ is a continuous function for $x \neq y$ and if there are numbers, $m$ and $a < 1$, such that $|k(x-y)| \leq m|x-y|^{-a}$ [33]. All of the kernels in this chapter satisfy one or the other of these conditions.

In general, the eigenvalues $\lambda$ of problem (17) are complex. If, however, the kernel is strictly positive, we can take advantage of Jentzsch's (1912) [37] theorem (see also [45] and [31]). This theorem is analogous to the Perron–Frobenius theorem for positive matrices. For our integral operator, it guarantees the existence of a simple, positive eigenvalue of largest modulus that dominates all other eigenvalues. The eigenfunction for this eigenvalue is positive. If the conditions of Jentzsch's theorem are met, the stability of trivial solution (11) changes as the dominant eigenvalue passes through $\lambda = 1$. For our problem, this occurs at the critical shift speed $c^*$.

The restriction that the kernel is strictly positive is important. If the kernel is only nonnegative, eigenvalues need not exist. If they do exist, the spectral radius of the operator $K$,

$$r(K) = \max_{\lambda_i \in \Lambda} |\lambda_i|, \tag{20}$$

is a (positive) eigenvalue with a nonnegative eigenfunction [38]. In this case, stability of the trivial solution is still lost through $\lambda = 1$.

All the redistribution kernels in this chapter are nonnegative. Continuous redistribution kernels with infinite support are positive and satisfy Jentzsch's theorem. Kernels with compact support need not satisfy this theorem. If, however, the radius of support is sufficiently large (relative to the patch size $L$ and speed $c$), Jentzsch's theorem does apply. We will soon find ourselves approximating kernels of infinite support with kernels of compact support. In these cases, we will try to choose parameters that guarantee that Jentzsch's theorem is still satisfied.

Previously, we [93] showed that eigenvalue problem (17) simplifies to a finite-dimensional problem in linear algebra if its kernel is separable. A separable kernel can be written as a finite sum, with each term in the sum the product of a function

of $x$ alone and a function of $y$ alone. Taking advantage of this fact, we determined the critical shift speed $c^*$ for a simple, separable toy problem.

Separable kernels are, however, rare. We now consider more general (numerical and analytical) methods that allow us to calculate the dominant eigenvalue and the critical shift speed $c^*$.

## 4 Numerical Approaches

One simple numerical approach for computing the dominant eigenvalue of problem (17) is the power method. As with matrix equations, the basic idea is to take an initial guess for the eigenvector and to repetitively rescale and iterate. More precisely, at each step of the process, we take our current estimate of the eigenfunction, $u_t(x)$, rescale this function using its sup norm over $D = [-L/2, L/2]$,

$$\tilde{u}_t(x) = \frac{u_t(x)}{\sup\limits_{x \in D} u_t(x)}, \tag{21}$$

and use the recurrence relation

$$u_{t+1}(x) = K[\tilde{u}_t(x)], \tag{22}$$

to obtain a new, improved estimate of our eigenfunction. Operator $K$, (19), accounts for both growth and dispersal. The dominant eigenvalue of the integral operator is now approximated by

$$\sup_{x \in D} u_t(x) \tag{23}$$

for large $t$. The power method is easy to implement, but it can be computationally inefficient.

More efficient approaches are based on Nyström's method [19,74]. For separable kernels, problem (17) simplifies to finding eigenvalues for a finite-dimensional matrix. It makes sense, therefore, to approximate our integral operator with a matrix. To do this, we first discretize our integral using a quadrature rule.

Let us consider, for example, the repeated trapezoidal rule. We divide the domain of integration, $[-L/2, L/2]$, into $N$ equal subintervals of length $\Delta y = L/N$. Replacing the variable $y$ in (17) with grid points

$$y_j = -\frac{L}{2} + j \cdot \Delta y, \qquad j = 0, 1, \ldots, N, \tag{24}$$

we approximate the integral in (17) using the trapezoidal rule,

$$\begin{aligned} \int_{-\frac{L}{2}}^{\frac{L}{2}} k(x + c - y)\, u(y)\, dy \;\approx\; & \frac{\Delta y}{2} \sum_{j=0}^{N-1} [\, k(x + c - y_j)\, u(y_j) \\ & + k(x + c - y_{j+1})\, u(y_{j+1})\,]. \end{aligned} \tag{25}$$

If we now evaluate the function $u(x)$ at the grid points $x_i = y_i$, $i = 0, 1, 2, \ldots, N$, eigenvalue problem (17) reduces to

$$\lambda\, u(x_i) = R_0\, \frac{\Delta y}{2} \sum_{j=0}^{N-1} [\, k(x_i + c - y_j)\, u(y_j) + k(x_i + c - y_{j+1})\, u(y_{j+1})\,]. \quad (26)$$

Finally, if we denote $u_i = u(x_i)$ and

$$\begin{aligned} A_{i0} &= \frac{\Delta x}{2}\, k(x_i + c - y_0), \\ A_{ij} &= \Delta x\, k(x_i + c - y_j), \qquad 1 \le j \le N-1, \\ A_{iN} &= \frac{\Delta x}{2}\, k(x_i + c - y_N), \end{aligned} \quad (27)$$

we obtain the finite-dimensional linear system

$$\lambda\, u_i = R_0 \sum_{j=0}^{N} A_{ij}\, u_j, \quad (28)$$

for $i = 0, \ldots, N$.

Thus, by employing Nyström's method, we transform the analysis of the dominant eigenvalue of an integral operator into the analysis of the dominant eigenvalue $\lambda$ of linear system (28).

We can now analyze linear system (28) in one of two ways. The first approach is to determine the eigenvalues of system (28) directly. The eigenvalues may be obtained using commands such as *eig*, *eigen*, or *spec* in computing environments such as MATLAB, R, or Scilab or by using well-known routines from numerical libraries such as *Numerical Recipes* [74], LAPACK [2], or the GNU Scientific Library [23]. These commands and routines commonly balance a matrix, reduce the balanced matrix to Hessenberg form, and find the eigenvalues of the Hessenberg matrix using a QR algorithm. Please see [74] for further details. Having found the eigenvalues, we now choose the dominant eigenvalue. Since this eigenvalue depends continuously on the parameters of the model, we can find the critical value for $c$, corresponding to $\lambda = 1$, using a standard root-finding algorithm, such as the method of bisection or Brent's method [9, 74].

As an alternative, set $\lambda$, in linear system (28), equal to one. Then, use an efficient algorithm, such as LU decomposition [74], to evaluate the determinant of the system. Finally, use a numerical root finder to locate the value of $c$ that makes the determinant zero. This last approach has the advantage of being simple to implement from scratch, but has the disadvantage that you are not guaranteed that $\lambda = 1$ is the dominant eigenvalue.

## 5 Analytic Approximations

In addition to solving for $c^*$ numerically, we want analytic estimates of the critical speed. The easiest way to obtain these estimates is to assume that the eigenfunction and the kernel in (17) can be approximated using single or double series of suitably chosen basis functions. These basis functions should be complete and linearly independent. Ideally, they should also be orthogonal. Obvious candidates include trigonometric functions (sines and cosines) and orthogonal polynomials such as Chebyshev, Hermite, Jacobi, Laguerre, or Legendre polynomials.

For convenience, we now expand the kernel $k(x + c - y)$ in the double series

$$k(x + c - y) \;=\; \sum_{i=0}^{\infty} \sum_{j=0}^{\infty} A_{ij}\;\; X_i(x)\, X_j(y)\,, \tag{29}$$

where $X_i(x)$ and $X_j(y)$ are Legendre polynomials relative to the interval $[-L/2,\; L/2]$. (Please see the appendix for a brief introduction to Legendre polynomials). The coefficients $A_{ij}$, which depend on $c$, are, by (96),

$$A_{ij} \;=\; \frac{(2i+1)\,(2j+1)}{L^2} \int_{-L/2}^{L/2} \int_{-L/2}^{L/2} k(x + c - y)\, X_i(x)\, X_j(y)\, dy\, dx\,. \tag{30}$$

If we insert expansion (29) into eigenvalue equation (17), we see that

$$\lambda\, u(x) \;=\; R_0 \sum_{i=0}^{\infty} \left( \sum_{j=0}^{\infty} A_{ij} \int_{-L/2}^{L/2} X_j(y)\, u(y)\, dy \right) X_i(x)\,. \tag{31}$$

We will treat this equation as an expansion of the eigenfunctions, $u(x)$, in Legendre polynomials relative to the interval $[-L/2,\; L/2]$,

$$u(x) \;=\; \sum_{i=0}^{\infty} a_i\;\; X_i(x)\,. \tag{32}$$

The coefficients $a_i$ clearly satisfy

$$a_i \;=\; \frac{R_0}{\lambda} \sum_{j=0}^{\infty} A_{ij} \int_{-L/2}^{L/2} X_j(y)\, u(y)\, dy\,, \quad i \;=\; 0, 1, 2, \ldots. \tag{33}$$

Expansion (32) presents the eigenfunctions as a linear combination of the orthogonal polynomials $X_i(x)$. If we use this expansion to eliminate $u(y)$ in coefficient equation (33), we see that

$$\lambda\, a_i \;=\; R_0 \sum_{j=0}^{\infty} A_{ij} \int_{-L/2}^{L/2} X_j(y) \sum_{k=0}^{\infty} a_k\, X_k(y)\, dy \tag{34}$$

$$= \; R_0 \sum_{k=0}^{\infty} \left( \sum_{j=0}^{\infty} A_{ij} \int_{-L/2}^{L/2} X_j(y)\, X_k(y)\, dy \right) a_k \; .$$

Since our Legendre polynomials are orthogonal and satisfy

$$\int_{-L/2}^{L/2} [X_i(x)]^2\, dx \;=\; \frac{L}{2i+1} \; , \tag{35}$$

it follows that

$$\lambda\, a_i \;=\; R_0\, L \sum_{j=0}^{\infty} \frac{A_{ij}}{2j+1}\, a_j \tag{36}$$

for $i = 0, 1, 2, ...$ and for $j = 0, 1, 2, ....$

System (36) is an infinite-dimensional system of linear algebraic equations for the eigenvalues $\lambda$ of the trivial solution. We can approximate the eigenvalues of largest modulus by truncating this system so that $i = 0, 1, ..., N$ and $j = 0, 1, ..., N$ for finite $N$. In many cases, $N$ need not be large.

Indeed, in some cases, $N = 0$ will suffice. For $N = 0$, we treat eigenfunctions, by (32), as constants,

$$u(x) \;\approx\; a_0\, X_0(x) \;=\; a_0 \; . \tag{37}$$

System (36), in turn, reduces to

$$\lambda\, a_0 \;\approx\; R_0\, L\, A_{00}\, a_0 \; . \tag{38}$$

After dividing both sides of this last equation by $a_0$, we obtain

$$\lambda \;\approx\; R_0\, L\, A_{00} \; , \tag{39}$$

where, by coefficient equation (30),

$$A_{00} \;=\; \frac{1}{L^2} \int_{-L/2}^{L/2} \int_{-L/2}^{L/2} k(x + c - y)\, dy\, dx \; . \tag{40}$$

At the critical speed $c = c^*$, $\lambda = 1$, and we conclude that

$$1 \;=\; \frac{R_0}{L} \int_{-L/2}^{L/2} \int_{-L/2}^{L/2} k(x + c^* - y)\, dy\, dx \; . \tag{41}$$

We can often use this last equation to obtain good estimates of the critical speed $c^*$.

We will refer to (39) as our $N = 0$ eigenvalue approximation. Equation (41) is our $N = 0$ critical-speed equation. The right hand side of these equations is the product of the net reproductive rate and the average dispersal success [56, 88, 89] of our shifted kernel.

A more precise estimate of the critical speed can be obtained by letting $N = 1$. For $N = 1$, we treat eigenfunctions as linear functions,

$$u(x) \approx a_0 X_0(x) + a_1 X_1(x) = a_0 + \frac{2a_1}{L} x . \tag{42}$$

System (36) now reduces to $N = 1$ approximation

$$\lambda \begin{bmatrix} a_0 \\ a_1 \end{bmatrix} = R_0 L \begin{bmatrix} A_{00} & \frac{A_{01}}{3} \\ A_{10} & \frac{A_{11}}{3} \end{bmatrix} \begin{bmatrix} a_0 \\ a_1 \end{bmatrix}. \tag{43}$$

At the critical speed, $c = c^*$, $\lambda = 1$, and we have that

$$\begin{bmatrix} R_0 L A_{00} - 1 & \frac{1}{3} R_0 L A_{01} \\ R_0 L A_{10} & \frac{1}{3} R_0 L A_{11} - 1 \end{bmatrix} \begin{bmatrix} a_0 \\ a_1 \end{bmatrix} = \begin{bmatrix} 0 \\ 0 \end{bmatrix}. \tag{44}$$

We want nontrivial eigenvectors, and so we require that this system be singular,

$$\begin{vmatrix} R_0 L A_{00} - 1 & \frac{1}{3} R_0 L A_{01} \\ R_0 L A_{10} & \frac{1}{3} R_0 L A_{11} - 1 \end{vmatrix} = 0. \tag{45}$$

This is our $N = 1$ critical-speed equation. It can be used to obtain improved estimates of the critical speed $c^*$.

We can proceed, in a similar way, for higher $N$. Often, however, low-order estimates of the critical speed do surprisingly well.

## 6 A Simple Example

We illustrate the above approximation scheme with a simple example. This is a toy problem that we have chosen for its analytic tractability. We will consider more realistic kernels in a later section.

Consider the symmetric, quadratic kernel

$$k(x) = \begin{cases} \dfrac{3}{4b}\left(1 - \dfrac{x^2}{b^2}\right), & |x| \le b, \\ 0, & |x| > b, \end{cases} \tag{46}$$

for $b > 0$. The coefficient at the front of this kernel has been chosen to guarantee that the kernel integrates to one.

If we add the restriction that

$$-b < x + c - y < b \tag{47}$$

for all $x$ and $y$ in the closed interval $[-L/2, L/2]$, our kernel is positive over the patch and the conditions for Jentzsch's theorem are satisfied. Eigenvalue problem (17) now reduces to

$$\lambda\, u(x) = R_0 \int_{-L/2}^{L/2} \frac{3}{4b}\left[1 - \frac{(x + c - y)^2}{b^2}\right] u(y)\, dy\ . \tag{48}$$

The kernel of this eigenvalue problem is, in fact, separable. It is easy to show that all eigenfunctions $u(x)$ of this problem are quadratic in $x$ and that system

$$\lambda \begin{bmatrix} a_0 \\ a_1 \\ a_2 \end{bmatrix} = R_0\, L \begin{bmatrix} A_{00} & \dfrac{A_{01}}{3} & \dfrac{A_{02}}{5} \\ A_{10} & \dfrac{A_{11}}{3} & \dfrac{A_{12}}{5} \\ A_{20} & \dfrac{A_{21}}{3} & \dfrac{A_{22}}{5} \end{bmatrix} \begin{bmatrix} a_0 \\ a_1 \\ a_2 \end{bmatrix}, \tag{49}$$

with coefficients

$$\begin{aligned} A_{00} &= \frac{3}{4b} - \frac{1}{8b^3}(L^2 + 6c^2), \\ A_{10} &= -\frac{3cL}{4b^3},\quad A_{01} = \frac{3cL}{4b^3}, \\ A_{20} &= -\frac{L^2}{8b^3},\quad A_{11} = \frac{3L^2}{8b^3},\quad A_{02} = -\frac{L^2}{8b^3}, \\ A_{21} &= A_{12} = A_{22} = 0 \end{aligned} \tag{50}$$

gives exact eigenvalues.

Nevertheless, (39) and (43) give us good approximations for the dominant eigenvalue. For $N = 0$ approximation (39),

$$\lambda \approx R_0\, L\, A_{00} = R_0\, L \left[\frac{3}{4b} - \frac{1}{8b^3}(L^2 + 6c^2)\right]. \tag{51}$$

Setting $\lambda = 1$ and solving for $c$ gives us

$$c^* \approx \pm\sqrt{b^2\left(1 - \frac{4b}{3R_0L}\right) - \frac{L^2}{6}}\,. \tag{52}$$

For two-row, two-column ($N = 1$) approximation (43),

$$\lambda \begin{bmatrix} a_0 \\ a_1 \end{bmatrix} = R_0\, L \begin{bmatrix} \frac{3}{4b} - \frac{1}{8b^3}(L^2 + 6c^2) & \frac{cL}{4b^3} \\ -\frac{3cL}{4b^3} & \frac{L^2}{8b^3} \end{bmatrix} \begin{bmatrix} a_0 \\ a_1 \end{bmatrix}, \tag{53}$$

the characteristic equation is

$$\lambda^2 + \frac{3R_0L}{4b^3}(c^2 - b^2)\lambda + \frac{R_0^2\, L^4}{64b^6}\left[6(c^2 + b^2) - L^2\right] = 0\,. \tag{54}$$

Setting $\lambda = 1$ and solving for $c$ gives us

$$c^* \approx \pm\sqrt{\frac{(R_0\, L^3 - 8\, b^3)(R_0\, L^3 - 6\, b^2\, R_0\, L + 8\, b^3)}{6\, R_0\, L\, (R_0\, L^3 + 8\, b^3)}}\,. \tag{55}$$

Finally, for $N = 2$, the characteristic equation is

$$\lambda^3 + \frac{3(c^2 - b^2)R_0\, L}{4\, b^3}\lambda^2 + \frac{3R_0^2\, L^4\left[5(c^2 + b^2) - L^2\right]}{160\, b^6}\lambda + \frac{R_0^3\, L^9}{2560\, b^9} = 0\,. \tag{56}$$

Setting $\lambda = 1$ and solving for $c$ gives us

$$c^* = \pm\sqrt{\frac{(8\, b^3 - R_0\, L^3)(R_0^2\, L^6 - 40\, b^3 R_0\, L^3 + 240\, b^5 R_0\, L - 320\, b^6)}{240\, b^3 R_0\, L(R_0\, L^3 + 8\, b^3)}}\,. \tag{57}$$

In Fig. 2, $N = 0$ approximation (52), $N = 1$ approximation (55), and the exact ($N = 2$) value of the critical speed, (57), are plotted against the net reproductive rate $R_0$. Since kernel (46) is symmetric, the curves in Fig. 4 are symmetric with respect to the $R_0$ axis. Shifting the patch to the right or left has the same effect on population persistence. For $N = 0$, (52) gives a good approximation to the true critical-speed curve for $R_0$ small. $N = 1$ approximation (55) is, in turn, visually indistinguishable from the exact critical-speed curve for both low and high values of $R_0$.

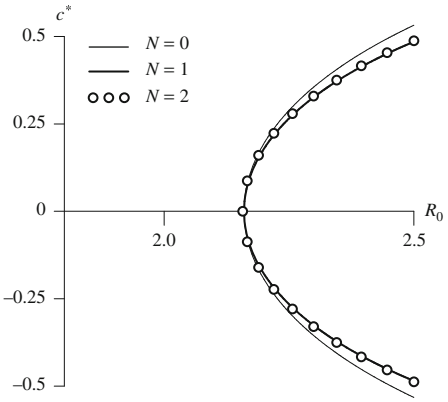


**Fig. 2** The critical speed $c^*$ plotted as a function of the net reproductive rate $R_0$ for quadratic kernel (46). The three curves depict $N = 0$ approximation (52), $N = 1$ approximation (55), and exact solution (57). Since kernel (46) is symmetric, these curves are symmetric about the $R_0$ axis. The $N = 1$ approximation is visually indistinguishable from the exact solution. Here, $b = 1.5$ km, and $L = 1$ km; we restricted $|c| < 0.5$ km/year in order to satisfy (47)

## 7 A Simplifying Approximation

In the above example, our $N = 0$ and $N = 1$ expansions both generated good estimates of the critical range-shift speed. Our kernel, moreover, were sufficiently simple that we could easily solve for $c^*$. For many kernels, unfortunately, it is much harder to solve for $c^*$.

For sufficiently smooth kernels, we will therefore expand the kernel $k(x + c - y)$ in a Taylor series in $c^* - y$. If the kernel is locally quadratic, we can then keep the first three terms in our Taylor series and approximate $c^*$ using the quadratic formula. We illustrate the procedure for $N = 0$. This procedure gives us a simple formula for $c^*$ that should be accurate for small critical speeds.

For $N = 0$,

$$\lambda \approx \frac{R_0}{L} \int_{-L/2}^{L/2} \int_{-L/2}^{L/2} k(x + c - y)\, dy\, dx\,. \tag{58}$$

Rewriting $k(x + c - y)$ as a Taylor series about $x$ yields

$$\lambda \approx \frac{R_0}{L} \sum_{n=0}^{\infty} \frac{1}{n!} \left[ \int_{-L/2}^{L/2} \int_{-L/2}^{L/2} k^{(n)}(x)(c - y)^n\, dy\, dx \right]. \tag{59}$$

If we keep the first three terms in the Taylor series and set $\lambda = 1$, we obtain

$$1 \approx R_0 \int_{-L/2}^{L/2} k(x)\,dx + \frac{R_0}{L} \int_{-L/2}^{L/2} k'(x)\,dx \left[ \int_{-L/2}^{L/2} (c^* - y) dy \right] \tag{60}$$

$$+ \frac{R_0}{L} \int_{-L/2}^{L/2} k''(x)\,dx \left[ \frac{1}{2} \int_{-L/2}^{L/2} (c^* - y)^2\,dy \right].$$

After calculating the integrals in $y$, we obtain the quadratic equation (in $c^*$)

$$\alpha c^{*2} + 2\beta c^* + \gamma + \frac{L^2\alpha}{12} - \frac{1}{R_0} \approx 0\,, \tag{61}$$

where

$$\alpha = \frac{1}{2}\left[ k'\left(\frac{L}{2}\right) - k'\left(-\frac{L}{2}\right)\right], \qquad \beta = \frac{1}{2}\left[ k\left(\frac{L}{2}\right) - k\left(-\frac{L}{2}\right)\right], \tag{62}$$

and

$$\gamma = \int_{-\frac{L}{2}}^{\frac{L}{2}} k(x)\,dx\,. \tag{63}$$

We can now use the quadratic formula to solve for the critical speed

$$c^* \approx -\frac{\beta}{\alpha} \pm \frac{1}{\alpha}\sqrt{\beta^2 - \alpha(\gamma + L^2\alpha/12 - 1/R_0)}\,. \tag{64}$$

The coefficient $\beta$ of the linear term in quadratic equation (61) vanishes when the kernel $k(x)$ is symmetric. Indeed, for symmetric kernels,

$$k\left(\frac{L}{2}\right) = k\left(-\frac{L}{2}\right), \qquad \text{and} \qquad k'\left(\frac{L}{2}\right) = -k'\left(-\frac{L}{2}\right). \tag{65}$$

Approximation (61) then reduces to

$$\alpha\, c^{*2} + \gamma + \frac{L^2\alpha}{12} - \frac{1}{R_0} \approx 0\,. \tag{66}$$

Solving for $c^*$, we obtain the remarkably simple formula

$$c^* \approx \pm\sqrt{\frac{1}{R_0\alpha} - \frac{\gamma}{\alpha} - \frac{L^2}{12}}\,. \tag{67}$$

Thus, for symmetric kernels, our quadratic approximation preserves the symmetry of $c^*$ with respect to $R_0$.

## 8 Realistic Kernels

Let us now apply our numerical procedures and/or our analytical approximations to some realistic redistribution kernels. We will look at three well-known workhorses: the Gaussian, Laplace, and Cauchy distributions. In addition, we will look at modified Bessel kernel (3).

### *8.1 Gaussian Distribution*

Let us first consider the Gaussian kernel

$$k(x) = \frac{1}{\sqrt{2\pi\sigma^2}} e^{-x^2/(2\sigma^2)} , \tag{68}$$

with standard deviation $\sigma > 0$. The Gaussian is the archetypal mesokurtic distribution; it has a special role in the theory of dispersal because of its strong connection to both the diffusion equation and the central limit theorem.

For this kernel, eigenvalue problem (17) reduces to

$$\lambda u(x) = R_0 \int_{-L/2}^{L/2} \frac{1}{\sqrt{2\pi\sigma^2}} e^{-(x+c-y)^2/(2\sigma^2)} u(y)\, dy . \tag{69}$$

The Gaussian kernel is not separable; we must, therefore, rely on numerical or analytical approximations to calculate the critical range-shift speed for this kernel [93].

Since kernel (68) is symmetric, let us first consider Taylor-series approximation (67). For this symmetric kernel,

$$\alpha = k'\left(\frac{L}{2}\right) = -\frac{L}{2\sigma^3\sqrt{2\pi}} e^{-L^2/(8\sigma^2)} \tag{70}$$

and

$$\gamma = \int_{-L/2}^{L/2} k(x)\, dx = \operatorname{erf}\left(\frac{\sqrt{2}L}{4\sigma}\right), \tag{71}$$

where the error function, $\operatorname{erf}(x)$, is given by the integral

$$\operatorname{erf}(x) = \frac{2}{\sqrt{\pi}} \int_0^x e^{-z^2}\, dz . \tag{72}$$

Formula (67) thus yields

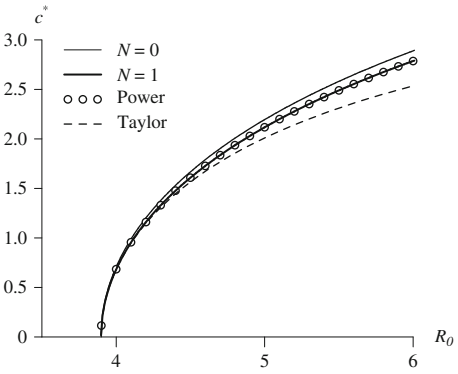


**Fig. 3** The critical speed $c^*$ plotted as a function of the net reproductive rate $R_0$ for Gaussian kernel (68). The four curves depict roots of $N = 0$ and $N = 1$ critical-speed equations (41) and (45), the numerical output of the power method, and Taylor-series approximation (73). Here, $\sigma = 3.0\,\text{km}$, and $L = 2.0\,\text{km}$. The $N = 0$ roots overestimate, but the $N = 1$ roots agree with, the power-method curve. Taylor-series approximation (73) provides good estimates of $c^*$ for small critical speeds, but underestimates $c^*$ for large critical speeds

$$c^* \approx \pm\sqrt{\frac{2\sigma^3\sqrt{2\pi}\left[R_0\,\text{erf}\left(\sqrt{2}\,L/(4\sigma)\right)-1\right]}{R_0\,L\,e^{-L^2/(8\sigma^2)}}-\frac{L^2}{12}}. \tag{73}$$

For the Gaussian distribution, we can no longer extract $c^*$ from critical-speed equations (41) and (45) analytically. We did, however, extract critical speeds from these equations numerically, for comparison, by evaluating the coefficients $A_{00}$, $A_{10}$, $A_{01}$, and $A_{11}$ as Riemann sums and by then solving for $c^*$ using a simple root-finding method, the method of bisection. The Riemann sums were calculated using a $100 \times 100$ grid; the method of bisection was run with a tolerance of $1 \times 10^{-6}$ .

Finally, we determined $c^*$ from eigenvalue problem (17) numerically, using both the power method and Nyström's method (see Sect. 4). For the power method, we iterated 250 times, for each value of $R_0$, using an FFT-assisted implementation of the extended trapezoidal rule with $2^{10}$ nodes. For Nyström's method, we used MATLAB's *eigs* command, with 100 grid points, and a root finder, the method of bisection, with tolerance $10^{-8}$. The two numerical approaches gave identical answers; we illustrate our results using output from the power method.

Figure 3 shows plots of the critical speed $c^*$, as a function of $R_0$, for a Gaussian kernel with standard deviation $\sigma = 3.0\,\text{km}$ and patch width $L = 2.0\,\text{km}$. The curves were obtained using, from top to bottom, $N = 0$ and $N = 1$ critical-speed equations (41) and (45), the power method, and Taylor-series approximation (73). Roots of the $N = 0$ equation slightly overestimate the true critical speed, but the roots of the $N = 1$ equation are visually indistinguishable from the numerical output of the power method. Taylor-series approximation (73) provides good estimates of $c^*$ for small critical speeds, but underestimates $c^*$ for large critical speeds.

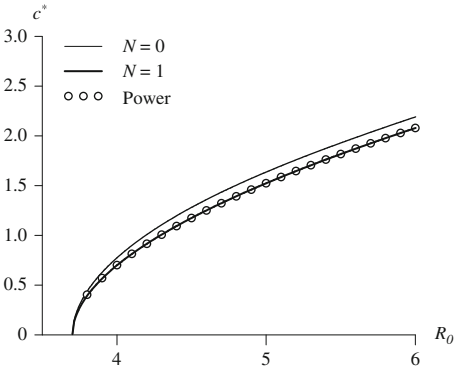


**Fig. 4** The critical speed $c^*$ plotted as a function of the net reproductive rate $R_0$ for Laplace kernel (74). The three curves depict roots of $N = 0$ and $N = 1$ critical-speed equations (41) and (45) and the numerical output of the power method. Here, $b = 3.0$ km, and $L = 2.0$ km. The $N = 0$ roots overestimate, but the $N = 1$ roots agree with, the power-method curve. Since the Laplace distribution is not differentiable at the origin, we do not plot a Taylor-series approximation for this example

## *8.2 Laplace Distribution*

The Laplace distribution,

$$k(x) = \frac{1}{2b} e^{-|x|/b} , \tag{74}$$

is a symmetric, leptokurtic dispersal kernel that is frequently encountered in empirical studies [e.g., 60,83,85]. It can also arise, in models, from a combination of diffusion and settling or advection and settling [57,63]. Kotz et al. [43] have written the definitive treatise analyzing the Laplace distribution from a statistical viewpoint.

For the Laplace distribution, eigenvalue problem (17) reduces to

$$\lambda u(x) = R_0 \int_{-L/2}^{L/2} \frac{1}{2b} e^{-|x+c-y|/b} u(y)\, dy . \tag{75}$$

Since the Laplace distribution is not separable and is not differentiable at the origin, we must rely on numerical methods to calculate the critical range-shift speed.

Figure 4 shows plots of the critical speed $c^*$, as a function of $R_0$, for a Laplace dispersal kernel with $b = 3.0$ km and patch width $L = 2.0$ km. These curves were obtained using (from top to bottom) $N = 0$ and $N = 1$ critical-speed equations (41) and (45) and the power method. Since the Laplace distribution is not differentiable at the origin, we do not plot Taylor-series approximation (67) for this distribution. The plotted curves were produced in the same manner as for the Gaussian kernel. Roots of the $N = 0$ equation slightly overestimate the true critical speed, but roots of the $N = 1$ equation are, once again, visually indistinguishable from the numerical output of the power method.

## 8.3 Cauchy Distribution

The Cauchy distribution,

$$k(x) = \frac{1}{\pi b\left(1 + \frac{x^2}{b^2}\right)}, \tag{76}$$

is a symmetric, fat-tailed distribution with no mean, variance, or higher moments. The Cauchy distribution, and related power law models, have proven important in studies of spore dispersal gradients [22], long-distance dispersal [82], and the spread of plant diseases [10, 58, 81].

For the Cauchy distribution, eigenvalue problem (17) reduces to

$$\lambda u(x) = R_0 \int_{-L/2}^{L/2} \frac{u(y)}{\pi b\left[1 + \frac{(x+c-y)^2}{b^2}\right]}\, dy\ . \tag{77}$$

Since the Cauchy distribution is not separable, we must rely on numerical or analytical approximations to calculate the critical range-shift speed.

In this instance,

$$\alpha = k'\left(\frac{L}{2}\right) = -\frac{bL}{\pi\left(b^2 + \frac{L^2}{4}\right)^2}\ . \tag{78}$$

and

$$\gamma = \int_{-L/2}^{L/2} k(x)\, dx = \frac{2}{\pi} \arctan\frac{L}{2b}\ . \tag{79}$$

Taylor-series approximation (67) now produces

$$c^* \approx \pm\sqrt{\frac{[2R_0 \arctan(L/2b) - \pi]\,(4b^2 + L^2)^2}{16\, R_0\, bL} - \frac{L^2}{12}}. \tag{80}$$

Figure 5 shows plots of the critical speed $c^*$, as a function of $R_0$, for a Cauchy dispersal kernel with $b = 2.0$ km and patch width $L = 2.0$ km. These curves were obtained using (from top to bottom) $N = 0$ and $N = 1$ critical-speed equations (41) and (45), the power method, and Taylor-series approximation (80). These curves were produced in the same manner as for the Gaussian kernel. Roots of the $N = 0$ equation slightly overestimate the true critical speed, but roots of the $N = 1$ equation are, once again, visually indistinguishable from the numerical output of the power method. The Taylor-series approximation, (80), once again provides good estimates of $c^*$ for small critical speeds, but underestimates $c^*$ for large critical speeds.

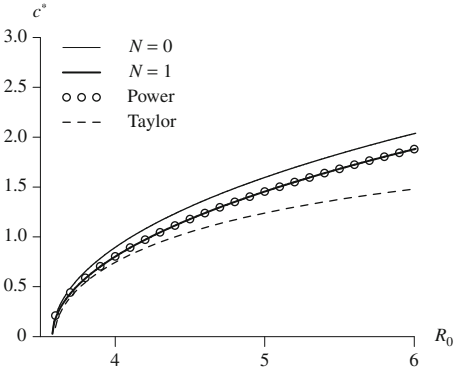


**Fig. 5** The critical speed $c^*$ plotted as a function of the net reproductive rate $R_0$ for Cauchy kernel (76). The four curves depict roots of $N = 0$ and $N = 1$ critical-speed equations (41) and (45), the numerical output of the power method, and Taylor-series approximation (80). Here, $b = 2.0\,\text{km}$, and $L = 2.0\,\text{km}$. The $N = 0$ roots overestimate, but the $N = 1$ roots agree with, the power-method curve. Taylor-series approximation (80) provides good estimates of $c^*$ for small critical speeds, but underestimates $c^*$ for large critical speeds

## *8.4 Modified Bessel Distribution*

The modified Bessel distribution,

$$k(x) = \frac{\alpha}{\pi} K_0(\alpha|x|), \tag{81}$$

arises as the marginal distribution of a 2D distribution whose 1D distribution of dispersal distances is the exponential distribution [94]. More generally, this distribution is the product distribution for two normally distributed variates [18, 21].

For this kernel, eigenvalue problem (17) reduces to

$$\lambda u(x) = R_0 \int_{-L/2}^{L/2} \frac{\alpha}{\pi} K_0\left(\alpha|x + c - y|\right)\, u(y)\, dy. \tag{82}$$

Since the modified Bessel distribution is not separable, we must again rely on numerical or analytical approximations to calculate the critical range-shift speed.

Figure 6 shows the critical speed $c^*$, as a function of $R_0$, for modified Bessel function (81) for $\alpha = 2.5,\ 6,\ 12\,\text{km}^{-1}$ and patch width $L = 0.5\,\text{km}$. These curves were obtained using Nystöm's method with MATLAB's *eigs* command, with 100 grid points, and a root finder, the method of bisection, with tolerance $10^{-8}$. The curves cross in several places and are consistent with the dynamics in Fig. 1.

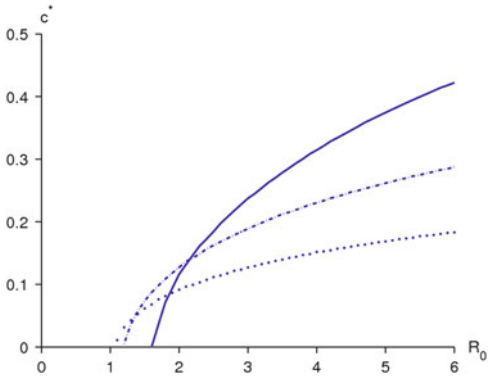


**Fig. 6** The critical speed $c^*$ plotted as a function of the net reproductive rate $R_0$ for modified Bessel kernel (81) and patch size $L = 0.5\,\text{km}$. The *solid curve* represents a vagile population ($\alpha = 2.5\,\text{km}^{-1}$), the *dot-dashed curve* represents an intermediate population ($\alpha = 6\,\text{km}^{-1}$), and the *dotted curve* is a sedentary population ($\alpha = 12\,\text{km}^{-1}$). The *dotted curve* has both a smaller $R_0$ intercept and a lower $c^*$ asymptote, implying that the sedentary population does comparatively better for small shift speeds but comparatively worse for high shift speeds. These *curves* were obtained using Nyström's method with MATLAB's *eigs* command, with 100 grid points, and a root finder, the method of bisection, with tolerance $10^{-8}$

## 9 Discussion

Climate change is altering the distributions of wildlife species at a fast rate. To estimate this rate, Loarie et al. [53] introduced and estimated an index of velocity of temperature change; this index has a global (geometric) mean of 0.42 km/year. Parmesan and Yohe [69], in turn, analyzed data for 1,700 species and estimated the average speed of significant poleward range shifts to be 6.1 km/decade. Can species keep up with this rate of climate change? In this chapter, we used an integrodifference equation to model the dynamics of a population that resides in a patch that shifts with speed $c$. In describing our model, we focused on butterflies, but our model can be applied to many animals and plants. We found that our model has a critical shift speed $c^*$ beyond which the population goes extinct. The critical shift speed $c^*$ depends sensitively on the dispersal ability of the species.

In Sect. 3, we reduced the problem of finding the critical shift speed $c^*$ to an eigenvalue problem. We then showed that $c^*$ can be estimated using numerical methods (Sect. 4) or analytical approximations (Sects. 5 and 7). Simple analytic approximations frequently yield results that are surprisingly close to numerical output. The biggest drawback of our analytical approach is that we must approximate our redistribution kernels with positive functions if we wish to satisfy Jentzsch's theorem. This positivity is easily broken.

Our analyses of the critical speed $c^*$ show that a species' dispersal ability has a profound but complicated impact on its success. When we plotted the critical speed $c^*$ with respect to the net reproductive rate $R_0$ for butterflies, in Sect. 8.4,

we found that the curves (for different dispersal parameters) cross at many points (Fig. 6). Sedentary populations do better (can survive for lower $R_0$) for low shift speeds, intermediate populations do better for intermediate shift speeds, and vagile populations do better at high shift speeds, but the loci of these transitions depend on where the curves intersect.

These observations suggest different conservation strategies for different dispersal classes. Sedentary species experiencing rapid habitat shifts may benefit from assisted dispersal. For vagile species experiencing slow habitat shifts but severe habitat fragmentation, restoration of degraded habitat may be of greater benefit.

The shape of the redistribution kernel also matters. The kernels in Figs. 3–5 have similar median absolute deviations (MAD $= \sigma/1.4826 = 2.02$, MAD $= b \ln 2 = 2.08$, and MAD $= b = 2$). In spite of this, if we superimpose the critical speed curves for the three kernels (data not shown), they intersect at numerous points. Cauchy distribution (76) and Laplace distribution (74) have smaller $R_0$ intercepts, presumably because more propagules pile up near the origin for these two distributions.

We hope to extend our analyses in new directions. In Sect. 3, we performed a linear stability analysis for the trivial solution $n^*(\bar{x}) = 0$. This was appropriate because we were only interested in population persistence. For more complicated growth functions, studying the stability of nontrivial traveling pulses may also reveal interesting dynamics. Needless to say, this is a harder problem. One must first determine the nontrivial pulse.

In addition, we have only analyzed a single-species model. Recent studies suggest that species-specific responses to climate change may sunder ecological communities [6, 79]. Studying multi-species models should thus prove interesting.

Finally, in our model, eggs hatch and grow and adults emerge only if they are in the climate-shifted patch for year $t$. Thus climate change only affects reproductive processes. We have built our model in this way because of the demonstrated effect of climate change on phenology and reproductive biology [14,24,50,59,68,90]. The observed dynamics could be quite different if climate change has a direct effect on dispersal. These are all interesting and open problems that merit future research.

## Appendix: Legendre Polynomials

The Legendre polynomials are the orthogonal polynomials formed by applying the Gram–Schmidt orthogonalization process to the functions $1, x, x^2, \ldots$ on the interval $[-1, 1]$ with the usual inner product. These polynomials are commonly used to approximate probability density functions (along with their derivatives, integrals, and convolutions) [3, 26, 52, 80] and to solve integral equations [46, 48, 91, 92].

The Legendre polynomials are given by

$$P_i(x) = \frac{1}{2^i i!} \frac{d^i}{dx^i} [(x^2 - 1)^i] \tag{83}$$

for $i = 0, 1, 2, \ldots$. The first few Legendre polynomials are

$$P_0(x) = 1\,, \quad P_1(x) = x\,, \quad P_2 = \frac{1}{2}(3x^2 - 1)\,, \quad P_3(x) = \frac{1}{2}(5x^3 - 3x)\,. \tag{84}$$

Additional Legendre polynomials can be generated using the recurrence relation

$$P_{i+1}(x) = \frac{2i+1}{i+1} x\, P_i - \frac{i}{i+1} P_{i-1}(x)\,. \tag{85}$$

The Legendre polynomials are even functions for $n$ even and odd functions for $i$ odd. Each of the $P_i(x)$ has $i$ distinct and real roots on the interval $(-1, 1)$. For our purposes, the most important property of the Legendre polynomials is that they form an orthogonal system on $[-1, 1]$ with

$$\int_{-1}^{1} P_i(x)\, P_j(x)\, dx = \frac{2}{2i+1} \delta_{ij}\,. \tag{86}$$

Here, $\delta_{ij}$ is the Kronecker delta, which equals 1 if $i = j$ and 0 if $i \neq j$.

Because the Legendre polynomials form a complete, orthogonal system over the interval $[-1, 1]$, we may expand a function $f(x)$ on this interval in a Legendre (or Fourier–Legendre) series of the form

$$f(x) = \sum_{i=0}^{\infty} a_i\, P_i(x)\,. \tag{87}$$

Please see [35,76] for convergence conditions. It is easy to show, using orthogonality condition (86), that the coefficients $a_i$ satisfy

$$a_i = \frac{2i+1}{2} \int_{-1}^{1} f(x)\, P_i(x)\, dx\,. \tag{88}$$

In a similar way, we can expand a bivariate function, $f(x, y)$, in a double series of the form

$$f(x, y) = \sum_{i=0}^{\infty} \sum_{j=0}^{\infty} A_{ij}\, P_i(x)\, P_j(y)\,. \tag{89}$$

The coefficients $A_{ij}$ in this series satisfy

$$A_{ij} = \frac{(2i+1)(2j+1)}{4} \int_{-1}^{1} \int_{-1}^{1} f(x, y)\, P_i(x)\, P_j(y)\, dy\, dx\,. \tag{90}$$

The problem that we are interested in (17), involves an integral over the interval $[-L/2, L/2]$. Rather than rescaling our problem, we find it convenient to follow [76] by introducing Legendre polynomials relative to the interval $[-L/2, L/2]$,

$$X_i(x) \;=\; P_i\left(\frac{2x}{L}\right). \tag{91}$$

In light of this transformation, our orthogonality condition, (86), now takes the form

$$\int_{-L/2}^{L/2} X_i(x)\, X_j(x)\, dx \;=\; \frac{L}{2i+1}\,\delta_{ij}\,. \tag{92}$$

When we write a function, $f(x)$, in a series of Legendre polynomials relative to the interval $[-L/2,\ L/2]$,

$$f(x) \;=\; \sum_{n=0}^{\infty} a_i\, X_i(x)\,, \tag{93}$$

the coefficients $a_i$ now satisfy

$$a_i \;=\; \frac{2i+1}{L}\int_{-L/2}^{L/2} f(x)\, X_i(x)\, dx\,. \tag{94}$$

Likewise, when we expand a bivariate function, $f(x,\ y)$, in a double series of Legendre polynomials relative to the interval $[-L/2,\ L/2]$,

$$f(x,\ y) \;=\; \sum_{i=0}^{\infty}\sum_{j=0}^{\infty} A_{ij}\, X_i(x)\, X_j(y)\,, \tag{95}$$

the coefficients $A_{ij}$ now satisfy

$$A_{ij} \;=\; \frac{(2i+1)\,(2j+1)}{L^2}\int_{-L/2}^{L/2}\int_{-L/2}^{L/2} f(x,\ y)\, X_i(x)\, X_j(y)\, dy\, dx\,. \tag{96}$$

## References


1. W.C. Allee, *The Social Life of Animals* (Norton, New York, 1938)
2. E. Anderson, Z. Bai, C. Bischof, S. Blackford, J. Demmel, J. Dongarra, J.D. Croz, A. Greenbaum, S. Hammarling, A. McKenney, D. Sorensen, *LAPACK User's Guide* (Society for Industrial and Applied Mathematics, Philadelphia, 1999)
3. R.D. Badinelli, Approximating probability density functions and their convolutions using orthogonal polynomials. Eur. J. Oper. Res. **95**, 211–230 (1996)
4. M. Bakkenes, J. Alkemade, F. Ihle, R. Leemans, J. Latour, Assessing effects of forecasted climate change on the diversity and distribution of European higher plants for 2050. Glob. Change Biol. **8**, 390–407 (2002)
5. H. Berestycki, O. Diekmann, C.J. Nagelkerke, P.A. Zegeling, Can a species keep pace with a shifting climate? Bull. Math. Biol. **71**, 399–429 (2009)

6. M.P. Berg, E.T. Kiers, G. Driessen, M. Van Der Heijden, B.W. Kooi, F. Kuenen, M. Liefting, H.A. Verhoef, J. Ellers, Adapt or disperse: understanding species persistence in a changing world. Glob. Change Biol. **16**, 587–598 (2010)
7. A.S. Best, K. Johst, T. Münkemüller, J.M. Travis, Which species will succesfully track climate change? The influence of intraspecific competition and density dependent dispersal on range shifting dynamics. Oikos **116**, 1531–1539 (2007)
8. R.J.H. Beverton, S.J. Holt, *On the Dynamics of Exploited Fish Populations* (Her Majesty's Stationery Office, London, 1957)
9. R.P. Brent, *Algorithms for Minimization Without Derivatives* (Prentice-Hall, Englewood Cliffs, 1973)
10. J.K.M. Brown, M.S. Hovmoller, Aerial dispersal of pathogens on the global and continental scales and its impact on plant disease. Science **297**, 537–541 (2002)
11. L.B. Buckley, Linking traits to energetics and population dynamics to predict lizard ranges in changing environments. Am. Nat. **171**, E1–E19 (2008)
12. M.B. Bush, H. Hooghiemstra, Tropical biotic responses to climate change, in *Climate Change and Biodiversity*, ed. by T.E. Lovejoy, L. Hannah (Yale University Press, New Haven, 2005), pp. 125–137
13. I.C. Chen, J.J. Shiu, B. Suzan, J.D. Holloway, V.K. Chey, H.S. Barlow, J.K. Hill, C.D. Thomas, Elevation increases in moth assemblages over 42 years on a tropical mountain. Proc. Natl. Acad. Sci. USA **106**, 1479–1483 (2009)
14. I. Chuine, Why does phenology drive species distribution? Phil. Trans. R. Soc. B **365**, 3149–3160 (2010)
15. R. Cousens, C. Dytham, R. Law, *Dispersal in Plants: A Population Perspective* (Oxford University Press, Oxford, 2008)
16. R.D. Cousens, When will plant morphology affect the shape of a seed dispersal "kernel"? J. Theor. Biol. **211**, 229–238 (2001)
17. M.J.R. Cowley, C.D. Thomas, D.B. Roy, R.J. Wilson, J.L. Leon-Cortes, D. Gutierrez, C.R. Bulman, R.M. Quinn, D. Moss, K.J. Gaston, Density-distribution relationships in British butterflies. I. The effect of mobility and spatial scale. J. Anim. Ecol. **70**, 410–425 (2001)
18. C.C. Craig, On the frequency function of xy. Ann. Math. Stat. **7**, 1–15 (1936)
19. L.M. Delves, J. Walsh, *Numerical Solution of Integral Equations* (Clarendon Press, Oxford, 1974)
20. R. Engler, A. Guisan, MIGCLIM: predicting plant distribution and dispersal in a changing climate. Divers. Distrib. **15**, 590–601 (2009)
21. B. Epstein, Some applications of the Mellin transform in statistics. Ann. Math. Stat. **19**, 370–379 (1948)
22. B.D.L. Fitt, P.H. Gregory, A.D. Todd, H.A. McCartney, O.C. MacDonald, Spore dispersal and plant disease gradients: a comparison between two empirical models. J. Phytopathol. **118**, 227–242 (1987)
23. M. Galassi, J. Davies, J. Theiler, B. Gough, G. Jungman, P. Aiken, M. Booth, F. Rossi, *GNU Scientific Library: Reference Manual* (Network Theory Ltd., Bristol, 2009)
24. K.J. Gaston, *The Structure and Dynamics of Geographic Ranges* (Oxford University Press, Oxford, 2003)
25. A. Guisan, W. Thuiller, Predicting species distribution: offering more than simple habitat models. Ecol. Lett. **8**, 993–1009 (2005)
26. P. Hall, Comparison of two orthogonal series methods of estimating a density and its derivatives on an interval. J. Multivar. Anal. **12**, 432–449 (1982)
27. S. Harrison, D. Murphy, P. Ehrlich, Distribution of the bay checkerspot butterfly, *Euphydryas editha bayensis*: Evidence for a metapopulation model. Am. Nat. **132**, 360–382 (1988)
28. A. Hastings, K. Higgins, Persistence of transients in spatially structured ecological models. Science **263**, 1133–1136 (1994)
29. R. Hickling, D.B. Roy, J.K. Hill, R. Fox, C.D. Thomas, The distributions of a wide range of taxonomic groups are expanding polewards. Glob. Change Biol. **12**, 450–455 (2006)

30. O. Honnay, K. Verheyen, J. Butaye, H. Jacquemyn, B. Bossuyt, M. Hermy, Possible effects of habitat fragmentation and climate change on the range of forest plant species. Ecol. Lett. **5**, 525–530 (2002)
31. T. Horiguchi, Y. Fukui, A variation of the Jentzsch theorem for a symmetric integral kernel and its application. Interdiscip. Inf. Sci. **2**, 139–144 (1996)
32. B. Huntley, North temperate responses, in *Climate Change and Biodiversity*, ed. by T. Lovejoy, L. Hannah (Yale University Press, New Haven, 2005), pp. 109–124
33. V. Hutson, J.S. Pym, *Applications of Functional Analysis and Operator Theory* (Academic, London, 1980)
34. IPCC, Climate Change 2007: Synthesis Report. Contribution of Working Groups I, II and III to the Fourth Assessment Report of the Intergovernmental Panel on Climate Change. Core Writing Team and R.K. Pachauri, A. Reisinger, IPCC, Geneva (2007)
35. D. Jackson, *The Theory of Approximation* (American Mathematical Society, New York, 1930)
36. C. Jeffree, E. Jeffree, Redistribution of the potential geographical ranges of mistletoe and Colorado beetle in Europe in response to the temperature component of climate change. Funct. Ecol. **10**, 562–577 (1996)
37. R. Jentzsch, Über integralgleichungen mit positivem kern. J. die Reine Angew. Math. **141**, 235–244 (1912)
38. S. Karlin, The existence of eigenvalues for integral operators. Trans. Am. Math. Soc. **113**, 1–17 (1964)
39. A.E. Kelly, M.L. Goulden, Rapid shifts in plant distribution with recent climate change. Proc. Natl. Acad. Sci. USA **105**, 11823–11826 (2008)
40. A. Komonen, A. Grapputo, V. Kaitala, J.S. Kotiaho, J. Päivinen, The role of niche breadth, resource availability and range position on the life history of butterflies. Oikos **105**, 41–54 (2004)
41. M. Kot, W.M. Schaffer, Discrete-time growth-dispersal models. Math. Biosci. **80**, 109–136 (1986)
42. M. Kot, M.A. Lewis, P. Van Den Driessche, Dispersal data and the spread of invading organisms. Ecology **77**, 2027–2042 (1996)
43. S. Kotz, T.J. Kozubowski, K. Podgorski, *The Laplace Distribution and Generalizations: A Revisit with Applications to Communications, Economics, Engineering, and Finance* (Birkhauser, Boston, 2001)
44. E. Kreyszig, *Introductory Functional Analysis with Applications* (Wiley, New York, 1978)
45. S. Krzemiński, Comment on 'A simple proof of the Perron–Frobenius theorem for positive symmetric matrices'. J. Phys. A. Math. Gen. **10**, 1437–1438 (1977)
46. H. Kschwendt, Numerical solution of integral equations using Legendre polynomials. J. Math. Phys. **10**, 1964–1968 (1969)
47. J. Latore, P. Gould, A.M. Mortimer, Spatial dynamics and critical patch size of annual plant populations. J. Theor. Biol. **190**, 277–285 (1998)
48. T.T. Lee, Y.F. Chang, Solutions of convolution integral and integral equations via double general orthogonal polynomials. Int. J. Syst. Sci. **19**, 415–430 (1988)
49. J. Lenoir, J.C. Gégout, P.A. Marquet, P. de Ruffray, H. Brisse, A significant upward shift in plant species optimum elevation during the 20th Century. Science **320**, 1768–1771 (2008)
50. T.M. Letcher, *Climate Change: Observed Impacts on Planet Earth* (Elsevier, Amsterdam, 2009)
51. M.A. Lewis, M.G. Neubert, H. Caswell, J.S. Clark, K. Shea, A guide to calculating discrete-time invasion rates from data, in *Conceptual Ecology and Invasions Biology: Reciprocal Approaches to Nature*, ed. by M.W. Cadotte, S.M. McMahon, T. Fukami (Springer, Dordrecht, 2006), pp. 169–192
52. X.B. Li, F.Q. Gong, A method for fitting probability distributions to engineering properties of rock masses using Legendre orthogonal polynomials. Struct. Saf. **31**, 335–343 (2009)
53. S. Loarie, P. Duffy, H. Hamilton, G.P. Asner, C.B. Field, D.D. Ackerly, The velocity of climate change. Nature **462**(24), 1052–1055 (2009)

54. D.R. Lockwood, A. Hastings, L.W. Botsford, The effects of dispersal patterns on marine reserves: does the tail wag the dog? Theor. Popul. Biol. **61**, 297–309 (2002)
55. F. Lutscher, Density-dependent dispersal in integrodifference equations. J. Math. Biol. **56**, 499–524 (2008)
56. F. Lutscher, M.A. Lewis, Spatially-explicit matrix models. J. Math. Biol. **48**, 293–324 (2004)
57. F. Lutscher, E. Pachepsky, M.A. Lewis, The effect of dispersal patterns on stream populations. SIAM J. Appl. Math. **65**, 1305–1327 (2005)
58. L.V. Madden, G. Hughes, F. van den Bosch, *The Study of Plant Disease Epidemics* (American Phytopathological Society, St. Paul, 2007)
59. J. McCarty, Ecological consequences of recent climate change. Conserv. Biol. **15**, 320–331 (2001)
60. T.E.X. Miller, B. Tenhumberg, Contributions of demography and dispersal parameters to the spatial spread of a stage-structured insect invasion. Ecol. Appl. **20**, 620–633 (2010)
61. D. Murphy, N. Wahlberg, I. Hanski, P.R. Ehrlich, Introducing checkerspots: Taxonomy and ecology, in *On the Wings of Checkerspots: A Model System for Population Biology*, ed. by P.R. Ehrlich, I. Hanski (Oxford University Press, Oxford, 2004), pp. 17–33
62. M.G. Neubert, H. Caswell, Demography and dispersal: calculation and sensitivity analysis of invasion speed for structured populations. Ecology **81**, 1613–1628 (2000)
63. M.G. Neubert, M. Kot, M.A. Lewis, Dispersal and pattern formation in a discrete-time predator-prey model. Theor. Popul. Biol. **48**, 7–43 (1995)
64. P. Opdam, D. Wascher, Climate change meets habitat fragmentation: linking landscape and biogeographical scale levels in research and conservation. Biol. Conserv. **117**, 285–297 (2004)
65. W.A. Ozinga, C. Römermann, R.M. Bekker, A. Prinzing, W.L.M. Tamis, J.H.J. Schaminée, S.M. Hennekens, K. Thompson, P. Poschlod, M. Kleyer, J.P. Bakker, J.M. van Groenendael, Dispersal failure contributes to plant losses in NW Europe. Ecol. Lett. **12**, 66–74 (2009)
66. C. Parmesan, Climate and species' range. Nature **382**, 765–766 (1996)
67. C. Parmesan, Detection at multiple levels: *Euphydryas editha* and climate change, in *Climate Change and Biodiversity*, ed. by T.E. Lovejoy, L. Hannah (Yale University Press, New Haven, 2005), pp. 56–60
68. C. Parmesan, Ecological and evolutionary responses to recent climate change. Annu. Rev. Ecol. Evol. Syst. **37**, 637–669 (2006)
69. C. Parmesan, G. Yohe, A globally coherent fingerprint of climate change impacts across natural systems. Nature **421**, 37–42 (2003)
70. C. Parmesan, N. Ryrholm, C. Stefanescu, J. Hill, C. Thomas, H. Descimon, B. Huntley, L. Kaila, J. Kullberg, T. Tammaru, W. Tennent, J. Thomas, M. Warren, Poleward shifts in geographical ranges of butterfly species associated with regional warming. Nature **399**, 579–583 (1999)
71. A.L. Perry, P.J. Low, J.R. Ellis, J.D. Reynolds, Climate change and distribution shifts in marine fishes. Science **308**, 1912–1915 (2005)
72. A.B. Potapov, M.A. Lewis, Climate and competition: the effect of moving range boundaries on habitat invasibility. Bull. Math. Biol. **66**, 975–1008 (2004)
73. J. Pöyry, M. Luoto, R.K. Heikkinen, M. Kuussaari, K. Saarinen, Species traits explain recent range shifts of Finnish butterflies. Glob. Change Biol. **15**, 732–743 (2009)
74. W.H. Press, S.A. Teukolsky, W.T. Vetterling, B.P. Flannery, *Numerical Recipes in C: The Art of Scientific Computing* (Cambridge University Press, Cambridge, 1992)
75. R.B. Primack, S.L. Miao, Dispersal can limit local plant distribution. Conserv. Biol. **6**, 513–519 (1992)
76. G. Sansone, *Orthogonal Functions* (Dover Publications, Mineola, 2004)
77. F.M. Schurr, G.F. Midgley, A.G. Rebelo, G. Reeves, P. Poschlod, S.I. Higgins, Colonization and persistence ability explain the extent to which plant species fill their potential range. Glob. Ecol. Biogeogr. **16**, 449–459 (2007)
78. M.W. Schwartz, Modelling effects of habitat fragmentation on the ability of trees to respond to climatic warming. Biodivers. Conserv. **2**, 51–61 (1992)

79. O. Schweiger, J. Settele, O. Kudrna, S. Klotz, I. Kühn, Climate change can cause spatial mismatch of trophically interacting species. Ecology **89**, 3472–3479 (2008)
80. T.A. Severini, *Elements of Distribution Theory* (Cambridge University Press, New York, 2005)
81. M. Shaw, Modeling stochastic processes in plant pathology. Annu. Rev. Phytopathol. **32**, 523–544 (1994)
82. M.W. Shaw, Simulation of population expansion and spatial pattern when individual dispersal distributions do not decline exponentially with distance. Proc. R. Soc. Lond. B **259**, 243–248 (1995)
83. C.A. Smith, I. Giladi, Y.S. Lee, A reanalysis of competing hypotheses for the spread of the California sea otter. Ecology **90**, 2503–2512 (2009)
84. V. Stevens, C. Turlure, M. Baguette, A meta-analysis of dispersal in butterflies. Biol. Rev. **85**, 625–642 (2010)
85. M.T. Tinker, D.F. Doak, J.A. Estes, Using demography and movement behavior to predict range expansion of the southern sea otter. Ecol. Appl. **18**, 1781–1794 (2008)
86. A. Trakhtenbrot, R. Nathan, G. Perry, D.M. Richardson, The importance of long-distance dispersal in biodiversity conservation. Divers. Distrib. **11**, 173–181 (2005)
87. J.M. Travis, Climate change and habitat destruction: a deadly anthropogenic cocktail. Proc. R. Soc. Lond. B **270**, 467–473 (2003)
88. R.W. Van Kirk, M.A. Lewis, Integrodifference models for persistence in fragmented habitats. Bull. Math. Biol. **59**, 107–137 (1997)
89. R.W. Van Kirk, M.A. Lewis, Edge permeability and population persistence in isolated habitat patches. Nat. Resour. Model. **12**, 37–64 (1999)
90. G. Walther, E. Post, P. Convey, A. Menzel, C. Parmesan, T. Beebee, J. Fromentin, O. Hoegh-Guldberg, F. Bairlein, Ecological responses to recent climate change. Nature **416**, 389–395 (2002)
91. M.L. Wanga, R.Y. Changa, S.Y. Yanga, Double generalized orthogonal polynomial series for the solution of integral equations. Int. J. Syst. Sci. **19**, 459–470 (1988)
92. S. Yalcinbas, M. Aynigul, T. Akkaya, Legendre series solutions of Fredholm integral equations. Math. Comput. Appl. **15**, 371–381 (2010)
93. Y. Zhou, M. Kot, Discrete-time growth-dispersal models with shifting species ranges. Theor. Ecol. **4**, 13–25 (2011)
94. Y. Zhou, M. Kot, The role of the modified Bessel distribution in dispersal models (2013) (in preparation)